Use of MEMS Cantilevers to Characterize Young's Modulus in Silicon-Rich Silicon Nitride

Sam Kendig, *skendig@mit.edu* - 6.152J/3.155J - Group D - 11/3/03

***Abstract*— Sample MEMS devices were developed, using cantilever and fixed-fixed beams from a silicon-rich silicon nitride film, and tested to determine physical properties of silicon-rich silicon nitride. By using a nano-indenter, we measured the deflection of the beams to a fixed load, to determine the physical bending stiffness of the silicon nitride film, from which the Young's modulus and residual stress could be extracted. Our data from the devices appears consistent with those in the literature, showing a Young's modulus of approximately 200 GPa, and a residual stress that can be on the order of 20-90 MPa. Analysis of this data confirms the strong dependence of bending stiffness on the geometries of the beams, and the importance of precisely measuring the critical features to produce accurate data.**

I. Introduction

WITH the increasing research into microelectromechanical systems (MEMS), physical properties of silicon and related materials have become as important as the previously relied upon electrical properties were to semiconductors. To develop mechanical systems on such a small scale, it is important to know how materials will react to the forces put upon them. Applications, such as MEMS used in atomic force microscopes, rely upon exact knowledge of these properties to function as desired.

In this work, we develop MEMS cantilevers and fixed-fixed beams to analyze mechanical properties of silicon-rich silicon nitride film on silicon substrate. By applying forces to these devices, we can measure the deflection, giving data from which we can calculate Young's modulus and residual stresses in the silicon nitride. These values are particularly important in developing MEMS devices, as Young's modulus determines how a material deforms with applied stress, and the residual stress determines how much additional stress can be applied to a device before it will yield or permanently deform.

II. Experiment

To begin the fabrication process, a 1μm layer of silicon-rich silicon nitride was grown in LPCVD. This layer was then measured to determine its thickness and refractive index. The refractive index was used to extract the ratio of silicon to nitrogen in the silicon nitride layer, which determines the physical properties that the film exhibits. The thickness was measured to be 1.02μm, very close to our expected growth of 1μm, and the refractive index of 2.3, indicating a silicon to nitrogen ratio between 4 and 6 [5]. Such a high ratio will cause the silicon nitride to have a thermal expansion coefficient closer to that of bulk silicon, reducing the residual stress caused by the differing contractions when the wafers cool.

After characterizing the silicon nitride layer, the wafer was prepared with a photoresist, and then exposed through contact lithography. Our masks created patterns for the cantilevers and the fixed-fixed beams in an array of lengths and widths. Once exposed, the photoresist was then developed to harden, preparing the wafer for etching. SF+6 plasma was used to etch the silicon nitride. The plasma reacts chemically with the silicon nitride to remove the areas revealed through the exposed photoresist. The photoresist was removed, and the finished result was inspected under an optical microscope to ensure that the wafer was fully etched. Measurements were also taken to find the new film thickness of the silicon nitride, measured at 0.99μm. The change in thickness is quite small, due to the protective layer of photoresist.

Once etched, the wafer was placed in a KOH bath. KOH was chosen for its planar selectivity, etching much faster in the <100> and <110> planes than in the <111> plane of silicon. This selectivity created an undercut, meaning the silicon beneath the silicon nitride cantilevers was etched away, leaving a silicon nitride film above an empty reservoir. After this final etch, the wafers were inspected again under an optical microscope, to ensure that the silicon beneath the cantilevers was fully removed.

The fully etched wafers were then tested using a nano-indenter, and data were taken on the loading versus deflection for various sizes of cantilevers and fixed-fixed beams. This data was then processed to extract values for Young's modulus and residual stress of silicon nitride.

III. Results & Discussion

Comparing the results from our data on the Young's modulus and residual stress in silicon nitride, we saw that our cantilevers compared closely to our expectations of stiffness, based upon moduli found in the literature [2]. Our fixed-fixed beams, however, had large deviations from the expected moduli. These deviations can be attributed to various errors and tolerances in our measurements. The fixed-fixed beams do have residual stresses consistent with those found by Sekimoto [5], when we use the appropriate modulus that we found from the cantilevers.

When analyzing the cantilever beams, we expect a linear relationship between the applied force and the deflection of the beam. Figures 1 and 2, show this relationship for both the $50\mu\text{m} \times 100\mu\text{m}$ and the $50\mu\text{m} \times 50\mu\text{m}$ cantilevers, as well as the linear fit that approximates the data. Based upon the sizes of these cantilevers, using the 1μm thickness that we measured earlier, we extracted a Young's modulus of 216GPa

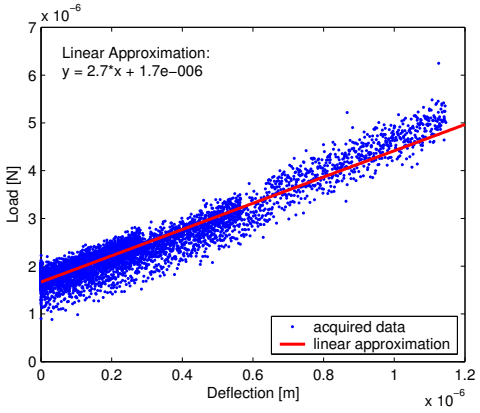

Fig. 1. Beam bending in a 50μm $\times$ 100μm cantilever with approximation based on linear bending stiffness. The cantilever has a stiffness of 2.7 N/m, correlating to a Young's modulus of 216GPa.

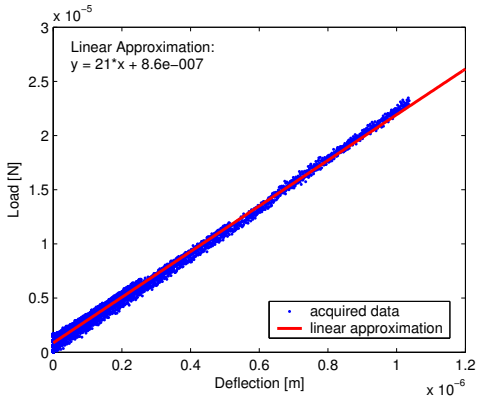

Fig. 2. Beam bending in a 50μm $\times$ 50μm cantilever with approximation based on linear bending stiffness. The cantilever has a stiffness of 21 N/m, correlating to a Young's modulus of 210GPa.

for the 100μm long cantilever, and a modulus of 210GPa for the 50μm one. These were very similar to the results found by Guo, who quoted a modulus of 195 $\pm$ 9GPa [2].

It is important to note how sensitive the modulus is to the geometry of the cantilevers. The modulus is proportional to the ratio of length to height raised to the third power. This means that a 10% error in one of these measurements can result in a 33% error in the calculation of the modulus. This seems particularly important when we consider that the nano-indenter has a tip radius of 10μm, and the indenter tip cannot rest exactly at the end of the cantilever without slipping off when it the cantilever bends. To compensate, we can consider the cantilever's length to be slightly less than its actual length, as the force is being applied to a point inward of the tip. This inward distance was on the order of 5μm, but could not be accurately measured, introducing error into the calculations. In the previous calculations for determining the Young's modulus of the 50μm $\times$ 100μm and 50μm $\times$ 50μm cantilevers, we used lengths of 95μm and 45μm for the 100μm and 50μm cantilevers, respectively. The uncertainty in the exact length, however, must be noted when considering the exactness of the modulus.

The third cantilever measured bore much poorer results than

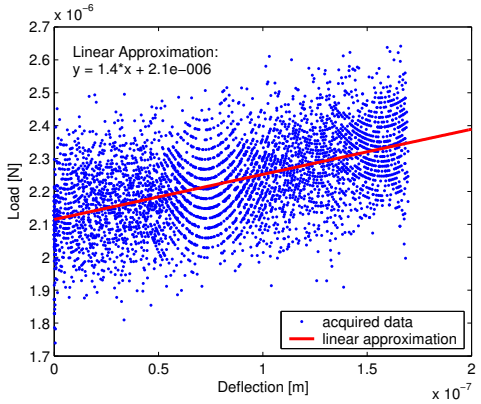

Fig. 3. Beam bending in a 50μm $\times$ 500μm cantilever, with linear approximation. Due to the high ratio of length to width, the beam produced very noisy data, with little correlation to the modulus. The fingerprint-like patterns are possibly due to resonant vibration modes of the beam.

the initial two, but deserves investigation. The beam measured 50μm $\times$ 500μm, a ratio of 10:1, much closer to classical studies of beam bending than the shorter beams we measured. However, the data, shown in Figure 3, does not correlate nearly as well as the data of the shorter, stiffer beams. The indenter attempts to find the surface of the cantilever by lowering its tip until it measures a 2μN force. In most cases, the deflection required to cause this is negligible, but with this long cantilever, the force does not reach 3μN before the indenter has reached its full extent. With such a long beam, small applied forces can create a great deal of deflection, such that the nano-indenter cannot resolve the forces before reaching the maximum allowed deflection. This produces a great deal of noisy data, with little correlation to Young's modulus.

One interesting feature to note in the longer cantilever is the very regular series of curves that develop in the seemingly noisy data. These curves are likely due to the cantilever resonating as it is depressed by the indenter tip. The oscillations produced are a function of the geometry and modulus of the cantilever, and are another means of determining the modulus of the silicon nitride film. A similar method using natural resonant frequencies was used by Guo in his determination of the modulus of silicon nitride [2].

While the cantilevers we manufactured provide a simple linear relationship between load and deflection, the fixed-fixed beams allow us to examine both modulus and residual stress in the silicon nitride. This relationship is not linear, but contains a third order term dependent only on Young's modulus and the beam geometry, and a first order term depending on Young's modulus, the residual stress, and the beam geometry. By matching this third order term, we can determine the modulus, and use it to find the residual stress. From the data in Figures 4 and 5, we calculated a modulus of 45GPa for the 5μm $\times$ 50μm beam, and a modulus of 49GPa for the 10μm $\times$ 50μm beam. These values are quite low when compared to the expected 195GPa.

One possible explanation for this discrepancy comes from the geometry of the beams. Since the beams are not perpendicular at their fixed edges, the boundary conditions may be

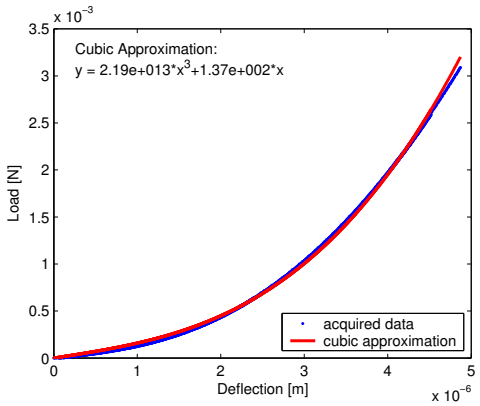

Fig. 4. Beam bending in a 5μm $\times$ 50μm fixed-fixed beam. The fitted cubic equation predicts a Young's modulus of 45GPa, and a residual stress of 14MPa.

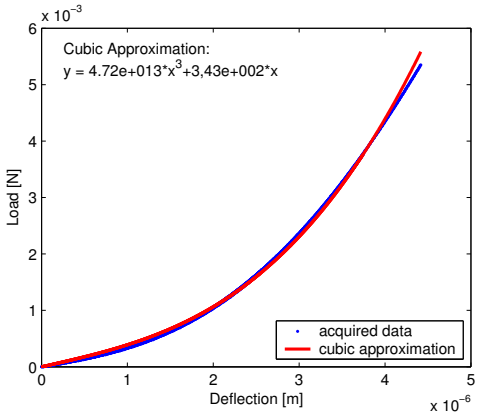

Fig. 5. Beam bending in a 10μm $\times$ 50μm fixed-fixed beam. The fitted cubic equation predicts a Young's modulus of 49GPa, and a residual stress of 84MPa.

changed slightly by interactions with the fixed regions. Also, if the tip of the indenter were not exactly at the center of the beams, the deflection would not be even on both sides. Both these effects would change the effective length of the beams. As with the cantilevers, the modulus is proportional to the cube of the length, so that any change in length greatly influences the calculated modulus. However, to account for the difference between the calculated modulus and the expected value, the effective length would have to be 60% longer than the beam's measured length. This seems unlikely, particularly given that placement of the indenter tip away from the center of the beam would decrease the effective length, making the beam stiffer and the modulus higher. It is also unlikely due to the fact that both measurements of the modulus are close in value to each other, while the random error in centering the indenter tip would imply less correlation between trials, producing more varying results.

Another possible explanation is that the beam begins to undergo plastic as well as elastic deformation as it is deflected further. When the deformations become non-reversible, in the plastic regime, our equations of deflection become less accurate. The plastic deformation will cause the beam to deflect more than we expect it to, resulting in what looks like a lower modulus.

If we assume a more standard Young's modulus than what we calculated from our fixed-fixed beams, we can examine the linear region, at small deflections, to determine the residual stress within the beams. This stress, calculated as 14MPa in the 5μm $\times$ 50μm beam and 84MPa in the 10μm $\times$ 50μm beam, is in rough agreement with Sekimoto's findings of residual stress ranging from 10-70MPa. If the residual stress becomes large enough, it starts to dominate the linear regime of the fixed-fixed beam bending, causing deflection to deviate from our predictions. However, for the 5μm $\times$ 50μm beam, we can safely ignore the effect of residual stresses less than 200MPa, and can ignore residual stresses in the 10μm $\times$ 50μm beams for values less than 3.1GPa. As silicon nitride has a yield stress on the order of 200MPa, residual stresses at these values would cause the fixed-fixed beams to fail, so this also puts a limit on the magnitude of acceptable residuals stresses. This factor drove the choice in using silicon-rich silicon nitride, as it has much lower residual stresses than standard stoichiometric silicon nitride.

IV. Conclusion

In this paper, we have shown how cantilever and beam bending can be used to determine Young's modulus and residual stress in materials for MEMS technologies. However, the oversensitivity of the Young's modulus calculations to errors in measuring the exact geometries of the features leads to an uncertainty that is higher than acceptable for anything beyond a first order approximation. To achieve a higher precision measurement of the modulus, more complex methods, such as resonance analysis, are required. For our purposes, these results show a close agreement with the existing literature, providing a simple method of determining modulus with linear and cubic models.

Acknowledgment

The author would like to thank Li-Wen Wang and Kostas Konistis for their help in lab.

References

[1] *3.155J/66.152J Lab Manual - Lab 2*. Fall 2003, MIT
[2] H. Guo and A. Lal, "Die-Level Characterization of Silicon-Nitride Membrane/Silicon Structures Using Resonant Ultrasonic Spectroscopy" in *Journal of Microelectromechanical Systems*, vol. 12, no. 1, February 2003, pp. 53-63.
[3] J. D. Plummer, M. D. Deal, P. B. Griffin, *Silicon VLSI Technology: Fundamentals, Practice, and Modeling*. Upper Saddle River, New Jersey: Prentice Hall, Inc., 2000.
[4] M. Schmidt and B. O'Handley, *3.155J/6.152J Lecture Notes*. Fall 2003, MIT
[5] M. Sekimoto, H. Yoshihara and T. Ohkubo, "Silicon Nitride Single-Layer X-Ray Mask" in *Journal of Vacuum Science Technology*, vol. 21, no. 4, November/December 1982, pp. 1017-1021.

APPENDIX I
DATA

APPENDIX II
CALCULATIONS